# A balloon-carried electrometer for high-resolution atmospheric electric field measurements in clouds

R. Giles Harrison

Citation: Rev. Sci. Instrum. **72**, 2738 (2001); doi: 10.1063/1.1369639
View online: http://dx.doi.org/10.1063/1.1369639
View Table of Contents: http://rsi.aip.org/resource/1/RSINAK/v72/i6
Published by the American Institute of Physics.

# A balloon-carried electrometer for high-resolution atmospheric electric field measurements in clouds

R. Giles Harrison[a)]
*Department of Meteorology, The University of Reading, P.O. Box 243, Earley Gate, Reading, Berks RG6 6BB, United Kingdom*

(Received 27 December 2000; accepted for publication 7 February 2001)

A disposable sensor for electric field measurements within clouds is described, which operates in conjunction with a standard meteorological radiosonde carried beneath a helium balloon. The radiosonde supplies telemetry and meteorological data. The sensor is constructed to measure electric fields of order 100 $\mathrm{V\,m^{-1}}$ and has been calibrated to 400 $\mathrm{V\,m^{-1}}$, typical of weakly electrified nonthunderstorm clouds. It measures using a regular cycle of measurement, dynamic zeroing, and marker pulses, which permits the integrity of the received data to be assessed. The electric field sensor is optically connected to the radiosonde, allowing it to remain electrically floating from the balloon system. A low-leakage electrometer switch for dynamic zeroing is an integral part of the system, and successful electric field measurements have been obtained aloft in temperatures down to $-60\,^{\circ}\mathrm{C}$. © *2001 American Institute of Physics.* [DOI: 10.1063/1.1369639]

## I. INTRODUCTION

Electric fields in the atmosphere under fair weather conditions are perturbed by aerosol particles,[1] which charge by diffusional capture of naturally produced ions.[2] Charge on atmospheric aerosol particles has been suggested to influence the formation of clouds, with possible climatic implications.[3] Although many electrical soundings of the atmosphere have been made during disturbed (thunderstorm) conditions, few such measurements have been made under less active atmospheric electrical conditions.[4] Previous soundings of atmospheric electric fields have shown that field changes occur at particulate boundaries,[5] but these measurements have not been continued and in-cloud measurements at low electric fields are rare.

Sensitive measurements of electric fields in clouds are troublesome because of the temperature and humidity variations a sensing device will encounter and the need for an aircraft or balloon platform. Sensors which have been used to measure electric field aloft include radioactive probes, field mills, and corona probes.[6] A disadvantage of radioactive probes is that ionization generated contributes to the local atmospheric space charge, complicating the measurement. Low noise field mill devices suitable for use at low field levels are precision devices and will usually require recovery after the flight. Corona probes are only suitable for use with large fields, and their absolute calibration is not straightforward if there are ventilation and pressure changes.

This low electric field detector has been developed to provide an inexpensive source of high temporal resolution in-cloud electrical measurements, when carried aloft by a helium meteorological balloon. The detector is disposable. It is operated in conjunction with a standard meteorological radiosonde (Vaisala type RS80) to record atmospheric data (temperature, pressure, and relative humidity) alongside the electrical measurements and provide the radio telemetry with which to retrieve the data. The modification to the telemetry used is sufficiently general that the same approach could be used with other (or additional) sensors by multiplexing.

## II. DESIGN

The electric field detector uses two spherical electrodes of diameter 2 cm, spaced 7.5 cm vertically apart, with the potential difference between the electrodes determined using an integral electrometer voltmeter. It hangs 10 m vertically beneath the radiosonde, which in turn hangs under the helium balloon, with a parachute attached for the descent. The voltage difference measured at the electrodes modulates a 100 kHz signal, applied, via an optical link, directly into the modulating stage of the radiosonde uhf transmitter. The optical isolation permits the measurement of electric fields independently of any potential on the sonde or the balloon on which it is flown. The electric field signal is recovered at the surface receiver, with the standard meteorological data unaffected (Fig. 1). The recovered signal is converted back to a voltage using a further phase-locked loop and logged at 20 Hz, together with information concerning the integrity of the link derived from the phase detector lock voltage.

Each electrode is constructed from a proprietary[7] polythene housing in two halves, with one half coated with conducting graphite paint. The electrodes are mounted on a polymer (Tufnol) frame for rigidity, using polytetrafluoroethylene (PTFE) insulators to prevent significant leakage currents flowing from charges on the support frame (Fig. 2). Connections between the electrometer circuit and the electrodes are made using a silver-loaded epoxy adhesive. The electrometer circuit is entirely housed within the lower electrode for protection and waterproofing: the unpainted half of the electrode housing is substantially hydrophobic, preventing the formation of water films causing current leakage between the sensing surface and the PTFE insulator.

a)Electronic mail: r.g.harrison@rdg.ac.uk

 

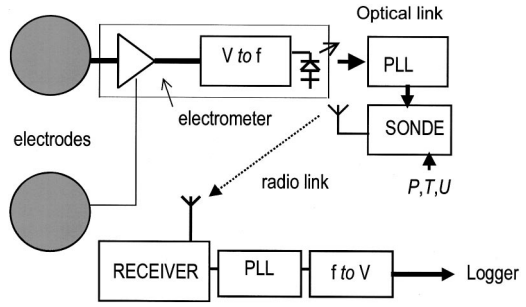


FIG. 1. Schematic of the electric field sensor using vertically spaced spherical electrodes. The electrometer circuit and batteries are mounted within the lower electrode, with the data conveyed via a voltage-to-frequency converter and an optical link operating at 100 kHz. A phase-locked loop (PLL) recovers the data from an optical receiver, and the signal is injected into a standard meteorological radiosonde measuring pressure *P*, temperature *T*, and relative humidity *U*. The uhf receiver recovers the 100 kHz signal, which a further PLL converts back to a voltage. The voltage is logged at 20 Hz by a computer and analog-to-digital converter.

The instrument supplies calibration information over the radio link. The electrometer measures for ~10 s, followed first by dynamic zeroing and then a greater than full-scale (marker) reading for approximately 1 s each. The received signal can therefore be compensated for changes in calibration with temperature by detecting the corresponding change in the dynamic zero.

## III. ELECTRONIC SYSTEM

The electronic system consists of an electrometer voltmeter stage as the front-end amplifier, together with zeroing circuitry. A master oscillator sequences the measurement and calibration cycles. The electrometer modulates a voltage-controlled oscillator to drive the optical link from which the signal is recovered and applied, via a driver stage, as frequency-modulation to the radiosonde transmitter. Figure 3 shows the schematic of the system. The majority of the circuit up to the optical transmitter is mounted within the lower electrode except for the photodetector: the optical receiver and signal recovery stages are mounted within the radiosonde.

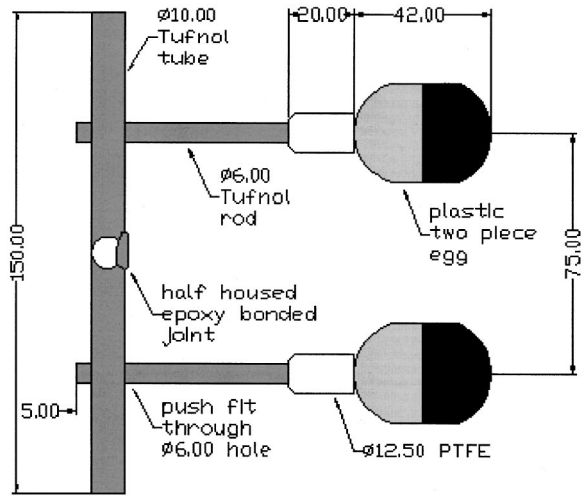


FIG. 2. Physical construction of the sensor. The sensing half of the polythene electrodes is coated in conducting graphite paint, with the uncoated half mounted using a PTFE stand-off on a Tufnol rod frame. The sensor hangs beneath the radiosonde and balloon. (Dimensions are in millimeters.)

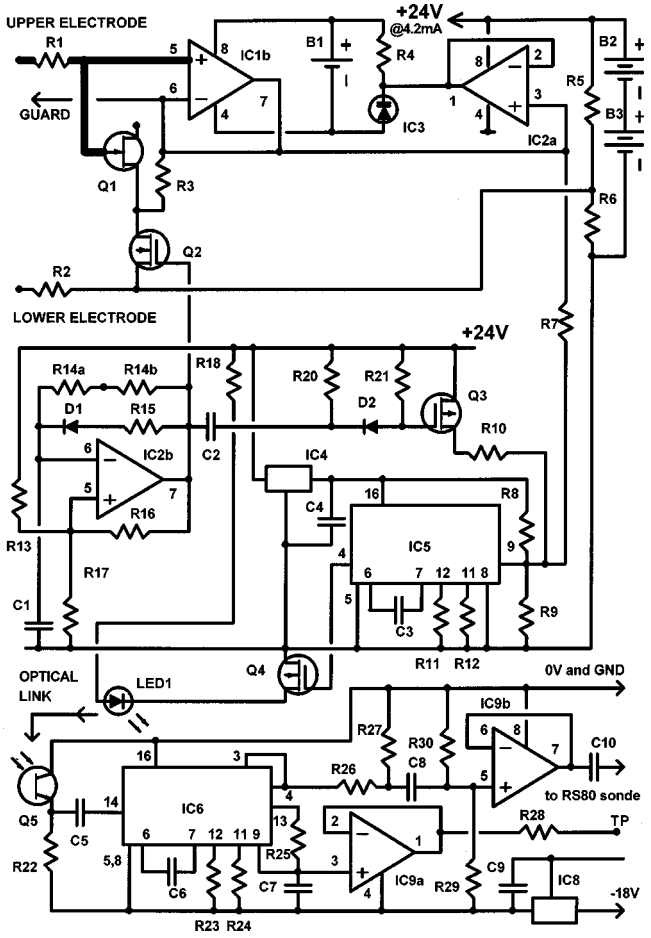


FIG. 3. Circuit schematic of the electrometer stage, voltage-to-frequency converter, and radiosonde driver stages. [*Components*: R1,2,20 1 MΩ; R3,6,10,16,17,13 10 KΩ; R4 200 KΩ; R5 91 KΩ; R7 120 KΩ; R8 39 KΩ; R9 24 KΩ; R11 30 KΩ; R12 470 KΩ; R14 10 MΩ+10 MΩ; R15 2M2; R18 68 KΩ; R19 68 KΩ; R21 10 MΩ; R22 820; R23 33 KΩ; R24 120 KΩ; R25 51 KΩ; R26 22 KΩ; R27 510; R28 100; R29,30 100 KΩ; C1,2 1 μF; C3 330 pF polystyrene; C4,8,9 100 nF; C5 10 nF; C6 330 pF polystyrene; C7 10 nF; IC1,7 LMC6042; IC2 OP290; IC3 TC04 (1.2 V reference); IC4 2950 (5 V regulator); IC5,6 4046 (pll); IC8 79L05; IC9 LMC6482; Q1 J113; Q2,4 VN10LP; Q3 ZVP3306A; Q5 SFH313FA (IR phototransistor); LED1 LD274 (IR emitter); B1 3 V Li cell; B2,B3 12 V minialkaline.]

### A. Electrometer stage

IC1b is wired as an extended-range electrometer voltage-follower[8] operated from 24 V battery supplies. The lower electrode is biased slightly above the negative terminal of the battery using the potential divider R5/R6, to allow small negative excursions of the upper electrode (with respect to the lower electrode), to be measured. During the dynamic zeroing phase of the operating cycle, the two electrodes are connected together by a solid-state ultrahigh-impedance switch comprising Q1 and Q2. Samples of the *j*FET devices used for Q1 (the J113) were investigated using a Keithley 6512 electrometer and found to have an ultralow gate-source current $i_{gs}$ for small gate-source bias voltages $v_{gs}$ (Fig. 4). A J113 device is accordingly deployed as the blocking element. In the zeroing mode, Q2 is switched on, and

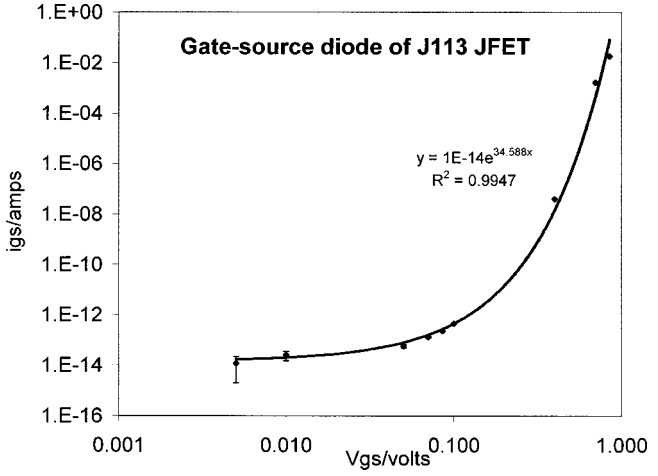


FIG. 4. Characteristics of the junction field effect transistor device (type J113) used in diode mode. This device is used as an ultralow leakage switch, with which the electrometer system is regularly zeroed.

Q1's $v_{gs}$ is then sufficient for it to conduct. In the measuring mode, Q2 is switched off, and the source of Q1 is guarded at the input potential of IC1b, to within the opamp's offset voltage (~2 mV) of Q1's gate. Figure 4 shows that, in this state, currents flowing through Q1 will be $\ll$10 fA. This approach has superior reliability at low temperatures, compared with mechanical switching implemented using reed switches.[9]

### B. Oscillator stages

The output of the voltage follower stage at IC2a is used to drive a voltage-controlled oscillator (VCO) constructed around IC5. It operates from a regulated 5 V supply (generated by IC4) with a nominal operating frequency range of 95–105 kHz, set by the value of C3, R11, and R12. This particular integrated circuit VCO is linear for input voltages between 3 and 5 V, thus the network R7-R8-R9 is used to shift the 0–24 V electrometer output into the restricted linear range. The output frequency is used to modulate the infrared emitter LED1, switched via Q4 from the unregulated battery supply.

IC2b provides a master oscillator for the entire system. It is a long-period (~10 s) oscillator, with an asymmetric mark-space ratio from the inclusion of D1 and R15. The short (~1 s) ''on'' pulse is used to zero the electrometer via the high impedance switch controlled by Q2, and a further short pulse is subsequently derived by differentiation (R20-C2), to operate Q3. Q3 switches the VCO input to the unregulated positive rail to give a frequency greater than full-scale output as a regular marker signal, which also permits remote monitoring of the battery voltage.

### C. Telemetry stages

The electrometer-modulated 100 kHz signal is received by infrared phototransistor Q5 and regenerated by phase-locked loop IC6. (The loop filter is also buffered by IC9a to provide a test point offering voltage variations proportional to the potential difference between the electrodes.) The regenerated square-wave from the phase-locked loop is reduced to 200 mV peak-to-peak (R26-R27), and rounded (C8-R30), before being ac coupled from driver stage IC9b to the radiosonde. The standard Vaisala RS80-15L radiosonde uses a 403 MHz radio frequency carrier, which is modulated by data from its meteorological sensors. It also carries a LORAN VLF (100 kHz) direction-finding (for position and wind determination) receiver. In this application the LORAN subsystem is removed from the RS80 radiosonde and the electric field sensor's narrow-band frequency-modulated (NBFM) signal at 100 kHz applied instead.

At the surface uhf radiosonde receiver, the 100 kHz NBFM signal is extracted by the commercial LORAN receiver circuitry and then applied to a further 100 kHz phase-lock loop similar to the circuitry around IC6 and IC9. The analog voltage present at the loop filter is buffered and digitized at 20 Hz using a 12-bit analog-to-digital converter, controlled via the parallel port of a laptop computer using a bespoke Turbo Pascal program. The standard meteorological data is received via the laptop computer's serial port, and the program interleaves the two asynchronous data streams and writes independent files of raw data from each source.

## IV. LABORATORY CALIBRATIONS

The sensor operates by measuring the displacement current arising from the changes in electric field sensed between the upper and lower electrodes as the instrument ascends on the balloon. This was verified by coating the inside of the upper electrode with conductive paint and driving it at a guard potential (equal to the potential of the outer surface), effectively eliminating the electrode capacitance $C$. There was then a minimal response of the sensor when subjected to external electric field changes.

The displacement current causes the potential of the upper electrode to change, according to the amount of charge transferred and the capacitance of the upper electrode. For a rate of change in electric field $dE/dt$, the displacement current causes the potential of the upper electrode to change at a rate $dV/dt$, where

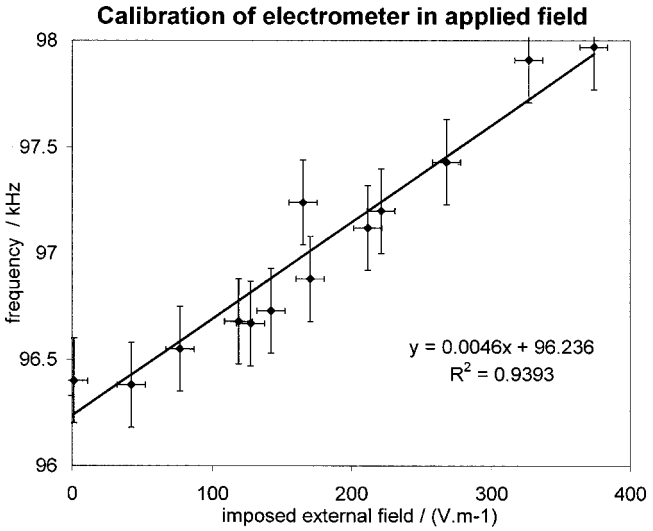


FIG. 5. Response of a prototype sensor to instantaneous changes in applied electric field, during the measurement cycle. The frequency recorded is the maximum frequency obtained immediately after the electric field is applied.

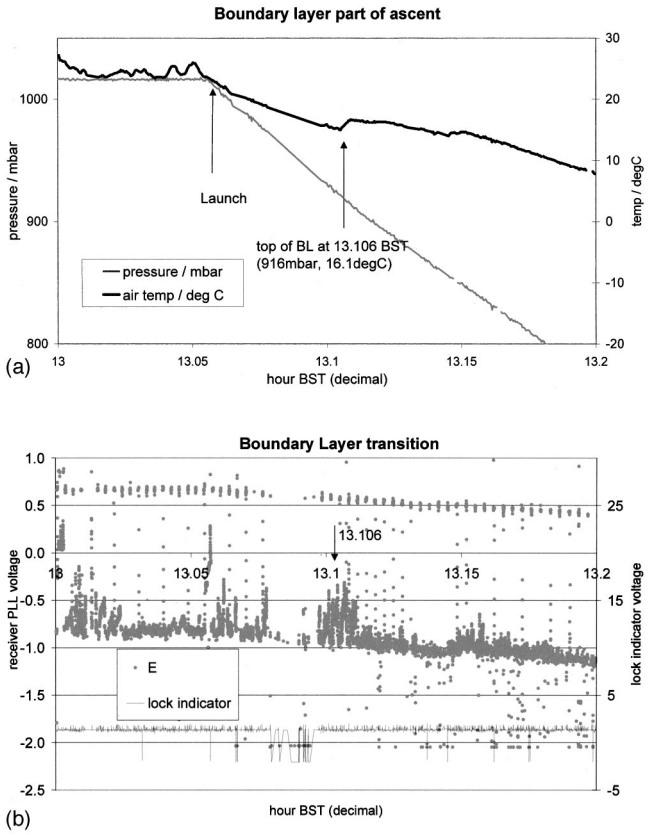


FIG. 6. Meteorological and electrical data obtained during an ascent made from reading in clear conditions, with the launch at 13.05 (decimal) h BST. (a) Meteorological measurements. Pressure and temperature determined from the RS80 radiosonde, with the boundary layer (BL) transition determined at 13.106 (decimal) h. (b) Electrical measurements. Recovered receiver phase-locked loop voltage showing the regular marker pulses, thermal drift, and electrical disturbance at the same time. (The PLL phase pulses are smoothed and also recorded as a measure of the data link's integrity: there is a brief period of poor signal after the launch during the boundary layer part of the ascent, associated with receiver overloading.)

$$C\frac{dV}{dt}=\varepsilon_0 A\frac{dE}{dt} \tag{1}$$

for an electrode capacitance $C$ and horizontal projected area $A$. The quantities $A$ and $C$ can be estimated theoretically, but are more usefully determined empirically for the individual construction of each sensor, by recording the change in potential for a change in an externally imposed potential gradient.

The calibration system consisted of two parallel plates, approximately square with sides of about 50 cm, mounted horizontally and vertically separated by 15 cm to allow the sensor to be suspended between them. Potential differences of between 0 and 60 V were applied to the two plates and the optical output of the battery-powered sensor system connected to a fast-response digital frequency meter. After the zeroing phase of the measurement cycle a potential difference was switched to the calibrating plates rapidly (when compared with the capacitance-limited rise in potential of the electrodes) and the maximum frequency reached was recorded. Figure 5 shows the response for a range of electric field changes, with the error bars arising from the repeated trials necessary to determine the maximum frequency and errors in the measurement of the dimensions from which the field was determined. The coefficients for a linear fit were individually derived for each device constructed.

## V. ATMOSPHERIC RESULTS

Basic atmospheric parameters can be used to confirm the operation of the device. A useful indication of correct operation is obtained when the instrument leaves the atmospheric boundary layer to emerge into the free troposphere. The boundary layer top (at typically 1 km) is associated with a transition in atmospheric aerosol number concentration. Under fair weather conditions, the aerosol becomes charged as a result of the vertical conduction current and ion-aerosol attachment.[10] Figure 6(a) shows meteorological data from a balloon launched in fine weather. The top of the boundary layer is clear from the temperature inversion marked. The corresponding raw electrical data obtained from the sensor is shown in Fig. 6(b). In the electric field time series, the electrometer voltage shows large transients as the sensor passes through the charged aerosol/clear air boundary. (It is also clear that there is a slow thermal drift in both the uncorrected zero and marker pulses.)

In practice, the instruments have continued to operate down to temperatures of $-60\,^{\circ}\mathrm{C}$ after emerging from water clouds as determined by the relative humidity sensor and temperature profiles, and intelligible signals have been recovered at physical distances over 30 km. Valid measurements are verified by the combination of clean marker pulses delimiting the measurement cycle, and steady lock-voltages from the receiving phase-locked loop.

## ACKNOWLEDGMENTS

The miniature printed circuit boards were constructed by A. G. Lomas and S. R. Tames. S. D. Gill and J. R. Knight supervised the balloon launches.

[1] W. A. Hoppel and S. G. Gathman, J. Appl. Phys. **41**, 1971 (1970).
[2] C. F. Clement and R. G. Harrison, J. Aerosol Sci. **24**, 481 (1992).
[3] R. G. Harrison, Space Sci. Rev. **94**, 381 (2000).
[4] W. Gringel, Ph.D. dissertation, Eberhard-Karls-Universität zu Tubingen, 1978 (unpublished).
[5] S. P. Venkiteshwaran, in *Recent Advances in Atmospheric Electricity*, Proceedings of the Second Wentworth Conference, edited by L. G. Smith (Pergamon, New York, 1958).
[6] D. R. McGorman and W. D. Rust, *The Electrical Nature of Storms* (Oxford University Press, New York, 1998).
[7] The housing is that originally supplied to house the small plastic toy contained within a children's confectionery *Kinder Surprise* 20 g chocolate egg (Ferrero UK Ltd., Awberry Court, Watford WD1 8YJ UK). The outer chocolate enclosure and foil coating must first be removed.
[8] R. G. Harrison, Rev. Sci. Instrum. **67**, 2636 (1996).
[9] R. G. Harrison and K. L. Aplin, Rev. Sci. Instrum. **71**, 4683 (2000).
[10] C. F. Clement and R. G. Harrison, J. Aerosol Sci. **31**, 363 (2000).